

Concealment by uniform motion

Tom G. Mackay¹ and Akhlesh Lakhtakia²

¹ School of Mathematics
 James Clerk Maxwell Building
 University of Edinburgh
 Edinburgh EH9 3JZ, UK
 email: T.Mackay@ed.ac.uk

² CATMAS — Computational & Theoretical Materials Sciences Group
 Department of Engineering Science & Mechanics
 212 Earth & Engineering Sciences Building
 Pennsylvania State University
 University Park, PA, 16802-6812, USA
 email: akhlesh@psu.edu

Abstract

The perceived lateral position of a transmitted beam, upon propagating through a slab made of homogeneous, isotropic, dielectric material at an oblique angle, can be controlled through varying the velocity of the slab. In particular, by judiciously selecting the slab velocity, the transmitted beam can emerge from the slab with no lateral shift in position. Thereby, a degree of concealment can be achieved. This concealment is explored in numerical calculations based on a 2D Gaussian beam.

Keywords: *Minkowski constitutive relations, moving slab, Gaussian beam, counterposition*

1 Introduction

The topic of invisibility — which is a very old one in optics and electromagnetics (Wolf & Habashy 1993) — has lately acquired a new lease of life with the advent of metamaterials (Fedotov, Mladyonov, Prosvirnin & Zheludev 2005; Alù & Engheta 2006). In a similar vein, it has recently been proposed that the exotic electromagnetic possibilities offered by metamaterials may be harnessed to achieve cloaking, at least in principle (Leonhardt 2006; Milton & Nicorovici 2006; Pendry, Schurig & Smith 2006). The theoretical arguments underlying this proposed cloaking are based on the facilitation of coordinate transformations by nonhomogeneous metamaterials.

A quite different approach to concealing a material is pursued in this paper. It is based on the perceived deflection of light by a material slab translating at constant velocity. No special material properties are required, but for illustrative purposes, we consider an isotropic, homogeneous, dielectric material. In two previous studies, we have demonstrated that the

much-heralded negative-phase-velocity phenomenon often associated with negatively refracting electromagnetic metamaterials can be realized by conventional materials through the process of uniform motion (Mackay & Lakhtakia 2004, 2006a). Here, we demonstrate that a substantial degree of concealment may also be realized by uniform motion.

As regards notational matters, 3 vectors are in boldface, with the $\hat{\cdot}$ symbol identifying unit vectors. Double underlining signifies a 3×3 dyadic and $\underline{\underline{I}}$ is the identity 3×3 dyadic. The superscript T denotes the transpose of a column vector. The permittivity and permeability of vacuum are ϵ_0 and μ_0 . The vacuum wavenumber is $k_0 = \omega\sqrt{\epsilon_0\mu_0}$ with ω being the angular frequency, and the vacuum wavelength is $\lambda_0 = 2\pi/k_0$.

2 Planewave propagation into a uniformly moving half-space

As a preliminary to concealment of a moving slab (§3), let us consider a uniformly moving half-space. Suppose that a plane wave is launched with wavevector $\mathbf{k}_i = k_i \hat{\mathbf{k}}_i$ from vacuum ($z < 0$) towards the half-space $z > 0$ occupied by an isotropic, nondissipative, dielectric material. This material moves at constant velocity $\mathbf{v} = v\hat{\mathbf{v}} = v\hat{\mathbf{x}}$, parallel to the interface and in the plane of incidence. In an inertial frame of reference that moves with the same velocity \mathbf{v} with respect to the laboratory frame of reference wherein \mathbf{k}_i is specified, the refracting material is characterized by relative permittivity ϵ_r . The Minkowski constitutive relations of the moving half-space in the laboratory frame of reference are (Chen 1983)

$$\left. \begin{aligned} \mathbf{D}(\mathbf{r}) &= \epsilon_0 \epsilon_r \underline{\underline{\alpha}} \cdot \mathbf{E}(\mathbf{r}) + \sqrt{\epsilon_0 \mu_0} (\mathbf{m} \times \underline{\underline{I}}) \cdot \mathbf{H}(\mathbf{r}) \\ \mathbf{B}(\mathbf{r}) &= -\sqrt{\epsilon_0 \mu_0} (\mathbf{m} \times \underline{\underline{I}}) \cdot \mathbf{E}(\mathbf{r}) + \mu_0 \underline{\underline{\alpha}} \cdot \mathbf{H}(\mathbf{r}) \end{aligned} \right\}, \quad (1)$$

where

$$\left. \begin{aligned} \underline{\underline{\alpha}} &= \alpha \underline{\underline{I}} + (1 - \alpha) \hat{\mathbf{v}}\hat{\mathbf{v}}, & \alpha &= \frac{1 - \beta^2}{1 - \epsilon_r \beta^2}, \\ \mathbf{m} &= m \hat{\mathbf{v}}, & m &= \frac{\beta(\epsilon_r - 1)}{1 - \epsilon_r \beta^2}, & \beta &= v\sqrt{\epsilon_0 \mu_0} \end{aligned} \right\}. \quad (2)$$

In order to exclude the possibility of evanescent plane waves, $\epsilon_r > 1$ is assumed. The envisaged scenario is illustrated schematically in Figure 1.

The angle ϕ_t between the refracted wavevector $\mathbf{k}_t = k_t \hat{\mathbf{k}}_t$, as observed from the laboratory frame of reference, and the unit vector $\hat{\mathbf{z}}$ normal to the interface is related to the angle of incidence $\phi_i = \cos^{-1}(\hat{\mathbf{k}}_i \cdot \hat{\mathbf{z}})$ by (Chen 1983)

$$\phi_t = \sin^{-1} \left(\frac{k_0 \sin \phi_i}{k_t} \right), \quad (3)$$

where

$$k_t = k_0 \left\{ 1 + \xi \left[1 - \beta (\hat{\mathbf{k}}_i \cdot \hat{\mathbf{v}}) \right]^2 \right\}^{1/2} \quad (4)$$

is the wavenumber of the refracted wave and $\xi = (\epsilon_r - 1)/(1 - \beta^2)$. Since $0 < \phi_t < \pi/2 \forall \phi_i \in (0, \pi/2)$, refraction is positive $\forall \beta \in (-1, 1)$ (Mackay & Lakhtakia 2006b).

The time-averaged Poynting vector of the refracted plane wave is given by (Chen 1983)

$$\mathbf{P}_t = P_t \hat{\mathbf{P}}_t = (|C_1|^2 + \epsilon_r |C_2|^2) (\mathbf{k}_t \times \hat{\mathbf{v}})^2 [\mathbf{k}_t + \xi \beta (k_0 - \beta \mathbf{k}_t \cdot \hat{\mathbf{v}}) \hat{\mathbf{v}}], \quad (5)$$

where C_1 and C_2 are constants, and the angle between $\hat{\mathbf{z}}$ and $\hat{\mathbf{P}}_t$ is

$$\phi_P = \tan^{-1} \left(\frac{\hat{\mathbf{P}}_t \cdot \mathbf{v}}{|v| \hat{\mathbf{P}}_t \cdot \hat{\mathbf{z}}} \right). \quad (6)$$

As an illustrative example, the angle ϕ_P is plotted in Figure 2 against $\beta \in (-1, 1)$ for $\phi_i \in \{15^\circ, 45^\circ, 75^\circ\}$, for the half-space characterized by $\epsilon_r = 6.0$. The orientation of the refracted time-averaged Poynting vector rotates towards the direction of motion as β increases from -1 . The counterposition regime — which occurs where $\phi_P < 0$ for $\phi_i > 0$ — is discussed elsewhere (Lakhtakia & McCall 2004; Mackay & Lakhtakia 2006b).

In connection with Figure 2, it is of particular interest here that $\phi_P = \phi_i$ at (i) $\beta = 0.08$ for $\phi_i = 15^\circ$, (ii) $\beta = 0.29$ for $\phi_i = 45^\circ$, and (iii) $\beta = 0.78$ for $\phi_i = 75^\circ$. That is, there exist angles of incidence at which the time-averaged Poynting vector is not deflected by the uniformly moving half-space. This suggests that it may be possible for a light beam — not to be confused with a plane wave — to pass through a uniformly moving slab at an oblique angle without experiencing a lateral shift in position. That suggestion inspired the research presented in the next section.

3 Beam propagation through a uniformly moving slab

Suppose that the uniformly moving half-space considered in §2 is now replaced by a slab of thickness L moving at constant velocity $\mathbf{v} = v\hat{\mathbf{x}}$ parallel to its two surfaces, as schematically illustrated in Figure 3. The slab — which is characterized, as before, by $\epsilon_r > 1$ in a co-moving reference frame — is immersed in vacuum.

A 2D beam with electric field phasor (Haus 1984)

$$\mathbf{E}_i(x, z) = \int_{-\infty}^{\infty} \mathbf{e}_i(\vartheta) \Psi(\vartheta) \exp[i(\mathbf{k}_i \cdot \mathbf{r})] d\vartheta, \quad z \leq 0 \quad (7)$$

is incident upon the slab at a mean angle θ_i relative to the slab normal direction $\hat{\mathbf{z}}$. The beam is represented as an angular spectrum of plane waves, with

$$\mathbf{k}_i = k_0 \left[\left(\vartheta \cos \theta_i + \sqrt{1 - \vartheta^2} \sin \theta_i \right) \hat{\mathbf{x}} - \left(\vartheta \sin \theta_i - \sqrt{1 - \vartheta^2} \cos \theta_i \right) \hat{\mathbf{z}} \right] \quad (8)$$

being the wavevector of each planewave contributor. The angular-spectral function $\Psi(\vartheta)$ is taken to have the Gaussian form (Haus 1984)

$$\Psi(\vartheta) = \frac{k_0 w_0}{\sqrt{2\pi}} \exp \left[-\frac{(k_0 w_0 \vartheta)^2}{2} \right], \quad (9)$$

with w_0 being the width of the beam waist. Two polarization states are considered: parallel to the plane of incidence, i.e.,

$$\mathbf{e}_i(\vartheta) \equiv \mathbf{e}_{\parallel} = \left(\vartheta \sin \theta_i - \sqrt{1 - \vartheta^2} \cos \theta_i \right) \hat{\mathbf{x}} + \left(\vartheta \cos \theta_i + \sqrt{1 - \vartheta^2} \sin \theta_i \right) \hat{\mathbf{z}} \quad (10)$$

and perpendicular to the plane of incidence, i.e.,

$$\mathbf{e}_i(\vartheta) \equiv \mathbf{e}_\perp = \hat{\mathbf{y}}. \quad (11)$$

The electric field phasor of the reflected beam is given as

$$\mathbf{E}_r(x, z) = \int_{-\infty}^{\infty} \mathbf{e}_r(\vartheta) \Psi(\vartheta) \exp[i(\mathbf{k}_r \cdot \mathbf{r})] d\vartheta, \quad z \leq 0, \quad (12)$$

with

$$\mathbf{k}_r = k_0 \left[\left(\vartheta \cos \theta_i + \sqrt{1 - \vartheta^2} \sin \theta_i \right) \hat{\mathbf{x}} + \left(\vartheta \sin \theta_i - \sqrt{1 - \vartheta^2} \cos \theta_i \right) \hat{\mathbf{z}} \right] \quad (13)$$

and

$$\mathbf{e}_r(\vartheta) = \begin{cases} r_{\parallel} \left[- \left(\vartheta \sin \theta_i - \sqrt{1 - \vartheta^2} \cos \theta_i \right) \hat{\mathbf{x}} \right. \\ \left. + \left(\vartheta \cos \theta_i + \sqrt{1 - \vartheta^2} \sin \theta_i \right) \hat{\mathbf{z}} \right] & \text{for } \mathbf{e}_i(\vartheta) = \mathbf{e}_{\parallel} \\ r_{\perp} \mathbf{e}_{\perp} & \text{for } \mathbf{e}_i(\vartheta) = \mathbf{e}_{\perp} \end{cases}. \quad (14)$$

The electric field phasor of the transmitted beam is given as

$$\mathbf{E}_t(x, z) = \int_{-\infty}^{\infty} \mathbf{e}_t(\vartheta) \Psi(\vartheta) \exp\{i[\mathbf{k}_t \cdot (\mathbf{r} - L\hat{\mathbf{z}})]\} d\vartheta, \quad z \geq L, \quad (15)$$

with $\mathbf{k}_t = \mathbf{k}_i$ and

$$\mathbf{e}_t(\vartheta) = \begin{cases} t_{\parallel} \mathbf{e}_i(\vartheta) & \text{for } \mathbf{e}_i(\vartheta) = \mathbf{e}_{\parallel} \\ t_{\perp} \mathbf{e}_{\perp} & \text{for } \mathbf{e}_i(\vartheta) = \mathbf{e}_{\perp} \end{cases}. \quad (16)$$

Expressions for the reflection coefficients $r_{\parallel, \perp}$ and transmission coefficients $t_{\parallel, \perp}$ are provided in equations (34)–(37) in the Appendix.

In view of Figure 2, we fixed the mean angle of incidence of the beam at $\theta_i = 45^\circ$ and explored the behaviour of the transmitted beam for $\beta < 0.29$, $\beta = 0.29$ and $\beta > 0.29$. The energy density of the beam in both half-spaces, as measured by

$$|\mathbf{E}|^2 = \begin{cases} |\mathbf{E}_i + \mathbf{E}_r|^2 & \text{for } z \leq 0 \\ |\mathbf{E}_t|^2 & \text{for } z \geq L \end{cases}, \quad (17)$$

is mapped for $z/\lambda_0 \in (-8, 12)$ and $x/\lambda_0 \in (-25, 25)$ in Figure 4 with the slab thickness $L = 4\lambda_0$. The restriction $\vartheta \in [-1, 1]$ was imposed to exclude evanescence. A beam waist of $w_0 = 1.75\lambda_0$ was selected for all calculations. We considered $\beta \in \{-0.15, 0.29, 0.8\}$ for both $\mathbf{e}_i = \mathbf{e}_{\parallel}$ and $\mathbf{e}_i = \mathbf{e}_{\perp}$.

Regardless of the polarization state, the transmitted beam does not undergo a lateral shift (relative to the incident beam) when $\beta = 0.29$. However, the transmitted beam is laterally shifted in the direction of $-\hat{\mathbf{x}}$ when $\beta < 0.29$ and in the direction of $+\hat{\mathbf{x}}$ when $\beta > 0.29$. The energy densities of the reflected and transmitted beams are sensitive to β and the polarization state of the incident beam.

A more quantitative representation of the transmitted beam is provided in Figure 5, wherein $|\mathbf{E}|^2$ is plotted against x for $\beta \in \{-0.15, 0.29, 0.8\}$ at $z = 4\lambda_0$. For comparison, $|\mathbf{E}|^2$ for the beam in the absence of the moving slab is also plotted. It is clear that the beam position for $\beta = 0.29$

coincides with the beam position in the absence of the moving slab. At $\beta = 0.29$, the peak energy density of the transmitted beam for the case of parallel polarization is approximately 11% less than it would be if the slab were absent; the corresponding figure for perpendicular polarization is 38%.

The median shift of transmitted beam in relation to the incident beam is defined as

$$\Delta = \left(\int_{-\infty}^{\infty} x |\mathbf{E}_t(x, L)|^2 dx \right) \left(\int_{-\infty}^{\infty} |\mathbf{E}_t(x, L)|^2 dx \right)^{-1} - \left(\int_{-\infty}^{\infty} x |\mathbf{E}_i(x, L)|^2 dx \right) \left(\int_{-\infty}^{\infty} |\mathbf{E}_i(x, L)|^2 dx \right)^{-1}. \quad (18)$$

For both parallel and perpendicular polarizations, Δ is plotted against $\beta \in (-1, 1)$ in Figure 6. Thus, regardless of the polarization state, the beam can be shifted laterally along $\pm \hat{\mathbf{x}}$ by means of uniform motion. In particular, the zero beam shift at $\beta = 0.29$ is further confirmed in Figure 6.

4 Concluding remarks

Our numerical investigations show that a 2D beam can pass obliquely through a uniformly moving slab without undergoing a lateral shift in its position. At a fixed angle of beam incidence, this effect occurs only for a unique translational slab velocity. However, extrapolating from Figure 2, for every angle of beam incidence a slab velocity can be found at which the beam undergoes no lateral shift. Furthermore, for a fixed angle of incidence, a pulsed beam will undergo zero lateral deflection, provided that the constitutive parameters do not vary with angular frequency in the pulse spectrum.

The degree of concealment achieved by uniform motion is not 100% due to reflections but, in the particular case of the example considered in §3, almost 90% of the peak energy density of the beam can be transmitted without deflection.

Acknowledgement: TGM is supported by a *Royal Society of Edinburgh/Scottish Executive Support Research Fellowship*.

Appendix

The reflection coefficients $r_{\parallel, \perp}$ and transmission coefficients $t_{\parallel, \perp}$ are straightforwardly calculated by solving the reflection-transmission problem as a boundary value problem. We outline the procedure here, further details being available elsewhere (Lakhtakia & Messier 2005).

Consider the plane wave with electric and magnetic field phasors

$$\left. \begin{aligned} \mathbf{E}(x, z) &= \tilde{\mathbf{e}}(z, \theta) \exp(ik_0 x \sin \theta) \\ \mathbf{H}(x, z) &= \tilde{\mathbf{h}}(z, \theta) \exp(ik_0 x \sin \theta) \end{aligned} \right\} \quad (19)$$

propagating in the xz plane. As in §3, a moving slab described by the Minkowski constitutive relations (1) occupies the region between $z = 0$ and $z = L$; elsewhere there is vacuum. We write

$$\tilde{\mathbf{p}}(z, \theta) = \tilde{p}_x(z, \theta) \hat{\mathbf{x}} + \tilde{p}_y(z, \theta) \hat{\mathbf{y}} + \tilde{p}_z(z, \theta) \hat{\mathbf{z}}, \quad (p = e, h). \quad (20)$$

Substitution of equations (1) and (19) into the source-free Maxwell curl postulates

$$\nabla \times \mathbf{E}(x, z) - i\omega \mathbf{B}(x, z) = \mathbf{0}, \quad (21)$$

$$\nabla \times \mathbf{H}(x, z) + i\omega \mathbf{D}(x, z) = \mathbf{0}, \quad (22)$$

delivers four differential equations and two algebraic equations. The latter two equations are easily solved for \tilde{e}_z and \tilde{h}_z . Thereby, the four differential equations may be expressed in matrix form as

$$\frac{\partial}{\partial z} [\mathbf{f}(z, \theta)] = ik_0 [\mathbf{P}(\theta)] [\mathbf{f}(z, \theta)], \quad (23)$$

where

$$[\mathbf{f}(z, \theta)] = \left[\tilde{e}_x(z, \theta), \tilde{e}_y(z, \theta), \tilde{h}_x(z, \theta), \tilde{h}_y(z, \theta) \right]^T \quad (24)$$

is a column vector and

$$\mathbf{P}(\theta) = \begin{bmatrix} 0 & 0 & 0 & \eta_0 \rho \\ 0 & 0 & -\eta_0 & 0 \\ 0 & -\epsilon_r \rho / \eta_0 & 0 & 0 \\ \epsilon_r / \eta_0 & 0 & 0 & 0 \end{bmatrix} \quad (25)$$

is a 4×4 matrix with

$$\rho = \alpha - \frac{(m + \sin \theta)^2}{\epsilon_r \alpha}. \quad (26)$$

The solution to (23) is conveniently expressed as

$$[\mathbf{f}(L, \theta)] = [\mathbf{M}(L, \theta)] [\mathbf{f}(0, \theta)], \quad (27)$$

in terms of the transfer matrix

$$[\mathbf{M}(L, \theta)] = \exp \{ ik_0 [\mathbf{P}(\theta)] L \}. \quad (28)$$

Now we turn to the incident, reflected and transmitted plane waves. Let the incident plane wave be represented in terms of linear polarization components as

$$\left. \begin{aligned} \tilde{\mathbf{e}}_i(z, \theta) &= [a_{\perp} \hat{\mathbf{y}} + a_{\parallel} (-\cos \theta \hat{\mathbf{x}} + \sin \theta \hat{\mathbf{z}})] \exp (ik_0 z \cos \theta) \\ \tilde{\mathbf{h}}_i(z, \theta) &= \eta_0^{-1} [a_{\perp} (-\cos \theta \hat{\mathbf{x}} + \sin \theta \hat{\mathbf{z}}) - a_{\parallel} \hat{\mathbf{y}}] \exp (ik_0 z \cos \theta) \end{aligned} \right\}, \quad z \leq 0. \quad (29)$$

The corresponding reflected and transmitted plane waves are given as

$$\left. \begin{aligned} \tilde{\mathbf{e}}_r(z, \theta) &= [a_{\perp} r_{\perp} \hat{\mathbf{y}} + a_{\parallel} r_{\parallel} (\cos \theta \hat{\mathbf{x}} + \sin \theta \hat{\mathbf{z}})] \exp (-ik_0 z \cos \theta) \\ \tilde{\mathbf{h}}_r(z, \theta) &= \eta_0^{-1} [a_{\perp} r_{\perp} (\cos \theta \hat{\mathbf{x}} + \sin \theta \hat{\mathbf{z}}) - a_{\parallel} r_{\parallel} \hat{\mathbf{y}}] \exp (-ik_0 z \cos \theta) \end{aligned} \right\}, \quad z \leq 0 \quad (30)$$

and

$$\left. \begin{aligned} \tilde{\mathbf{e}}_t(z, \theta) &= [a_{\perp} t_{\perp} \hat{\mathbf{y}} + a_{\parallel} t_{\parallel} (-\cos \theta \hat{\mathbf{x}} + \sin \theta \hat{\mathbf{z}})] \exp [ik_0(z - L) \cos \theta] \\ \tilde{\mathbf{h}}_t(z, \theta) &= \eta_0^{-1} [a_{\perp} t_{\perp} (-\cos \theta \hat{\mathbf{x}} + \sin \theta \hat{\mathbf{z}}) - a_{\parallel} t_{\parallel} \hat{\mathbf{y}}] \exp [ik_0(z - L) \cos \theta] \end{aligned} \right\}, \quad z \geq L, \quad (31)$$

respectively. By application of the boundary conditions at $z = 0$ and $z = L$ to the solution (27), the reflection and transmission coefficients are found to be related by the matrix algebraic equation

$$[\mathbf{K}(\theta)] [t_{\perp}, t_{\parallel}, 0, 0]^T = [\mathbf{M}(L, \theta)] [\mathbf{K}(\theta)] [1, 1, r_{\perp}, r_{\parallel}]^T, \quad (32)$$

wherein

$$\mathbf{K}(\theta) = \begin{bmatrix} 0 & -\cos \theta & 0 & \cos \theta \\ 1 & 0 & 1 & 0 \\ -\eta_0^{-1} \cos \theta & 0 & \eta_0^{-1} \cos \theta & 0 \\ 0 & -\eta_0^{-1} & 0 & -\eta_0^{-1} \end{bmatrix}. \quad (33)$$

Thus, after some manipulation, the reflection and transmission coefficients emerge as

$$r_{\perp} = \frac{(\cos^2 \theta - \epsilon_r \rho) \sin(k_0 L \sqrt{\epsilon_r \rho})}{(\cos^2 \theta + \epsilon_r \rho) \sin(k_0 L \sqrt{\epsilon_r \rho}) + 2i\sqrt{\epsilon_r \rho} \cos(k_0 L \sqrt{\epsilon_r \rho}) \cos \theta}, \quad (34)$$

$$r_{\parallel} = \frac{(\rho - \epsilon_r \cos^2 \theta) \sin(k_0 L \sqrt{\epsilon_r \rho})}{(\epsilon_r \cos^2 \theta + \rho) \sin(k_0 L \sqrt{\epsilon_r \rho}) + 2i\sqrt{\epsilon_r \rho} \cos(k_0 L \sqrt{\epsilon_r \rho}) \cos \theta}, \quad (35)$$

$$t_{\perp} = \frac{-2i\sqrt{\epsilon_r \rho} \cos \theta}{(\cos^2 \theta + \epsilon_r \rho) \sin(k_0 L \sqrt{\epsilon_r \rho}) + 2i\sqrt{\epsilon_r \rho} \cos(k_0 L \sqrt{\epsilon_r \rho}) \cos \theta}, \quad (36)$$

$$t_{\parallel} = \frac{2i\sqrt{\epsilon_r \rho} \cos \theta}{(\epsilon_r \cos^2 \theta + \rho) \sin(k_0 L \sqrt{\epsilon_r \rho}) + 2i\sqrt{\epsilon_r \rho} \cos(k_0 L \sqrt{\epsilon_r \rho}) \cos \theta}. \quad (37)$$

References

- [1] Alù, A. & Engheta, N. 2005 Achieving transparency with plasmonic and metamaterial coatings. *Phys. Rev. E* **72**, 016623. Erratum: 2006 **73**; 019906(E).
- [2] Chen, H.C. 1983 *Theory of electromagnetic waves*. New York, NY, USA: McGraw–Hill.
- [3] Fedotov, V.A., Mladyonov, P.L., Prosvirnin, S.L & Zheludev, N.I. 2005 Planar electromagnetic metamaterial with a fish scale structure. *Phys. Rev. E* **72**, 056613.
- [4] Haus, H.A. 1984 *Waves and fields in optoelectronics*. Englewood Cliffs, NJ, USA: Prentice–Hall.
- [5] Lakhtakia, A. & McCall, M.W. 2004 Counterposed phase velocity and energy–transport velocity vectors in a dielectric–magnetic uniaxial medium. *Optik* **115**, 28–30.
- [6] Lakhtakia A. & Messier R. 2005 *Sculptured thin films*. Bellingham, WA, USA: SPIE Press.
- [7] Leonhardt, U. 2006 Optical conformal mapping. *Science* **312**, 1777–1780.
- [8] Mackay, T.G. & Lakhtakia, A. 2004 Negative phase velocity in a uniformly moving, homogeneous, isotropic, dielectric–magnetic medium. *J. Phys. A: Math. Gen.* **37**, 5697–5711.
- [9] Mackay, T.G. & Lakhtakia, A. 2006a On electromagnetics of an isotropic chiral medium moving at constant velocity *Proc. R. Soc. Lond. A* (to appear).
- [10] Mackay, T.G. & Lakhtakia, A. 2006b Counterposition and negative refraction due to uniform motion. <http://arxiv.org/abs/physics/0610039>

- [11] Milton, G.W. & Nicorovici, N-A. P. 2006 On the cloaking effects associated with anomalous localized resonance. *Proc. R. Soc. Lond. A* **462**, 3027–3059.
- [12] Pendry, J.B., Schurig, D. & Smith, D.R. 2006 Controlling electromagnetic fields. *Science* **312**, 1780–1782.
- [13] Wolf, E. & Habashy, T. 1993 Invisible bodies and uniqueness of the inverse scattering problem. *J. Mod. Optics* **40**, 785–792.

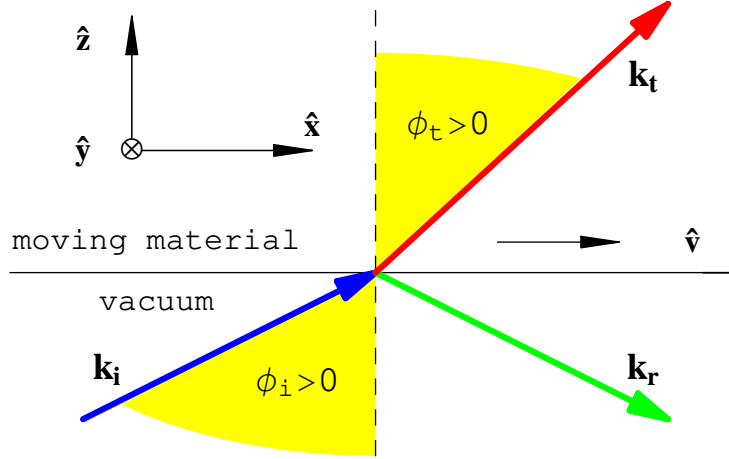


Figure 1: A plane wave with wavevector \mathbf{k}_i is incident from vacuum onto a half-space occupied by a simply moving dielectric material at an angle ϕ_i with respect to the unit vector $\hat{\mathbf{z}}$ normal to the planar interface. The moving material is characterized by relative permittivity $\epsilon_r > 0$ in a co-moving frame of reference. As observed in the non-co-moving (laboratory) frame of reference wherein the incident plane wave is specified, the refracted wavevector \mathbf{k}_t makes an angle ϕ_t with $\hat{\mathbf{z}}$.

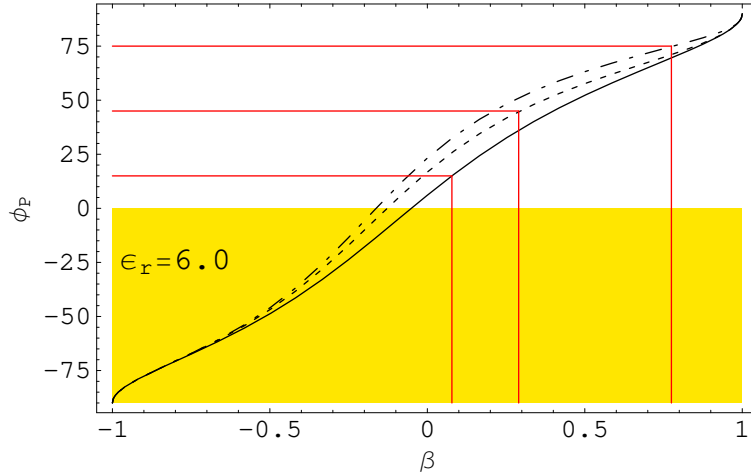


Figure 2: The angle ϕ_P (in degree) between the time-averaged Poynting vector \mathbf{P}_t and the unit vector $\hat{\mathbf{z}}$, plotted as a function of $\beta \in (-1, 1)$, when the angle of incidence $\phi_i = 15^\circ$ (solid curve), 45° (dashed curve) and 75° (broken dashed curve); and $\epsilon_r = 6.0$. The red lines indicate where $\phi_P = \phi_i$. The counterposition regime $\{\phi_P < 0^\circ, \phi_t > 0^\circ\}$ is shaded.

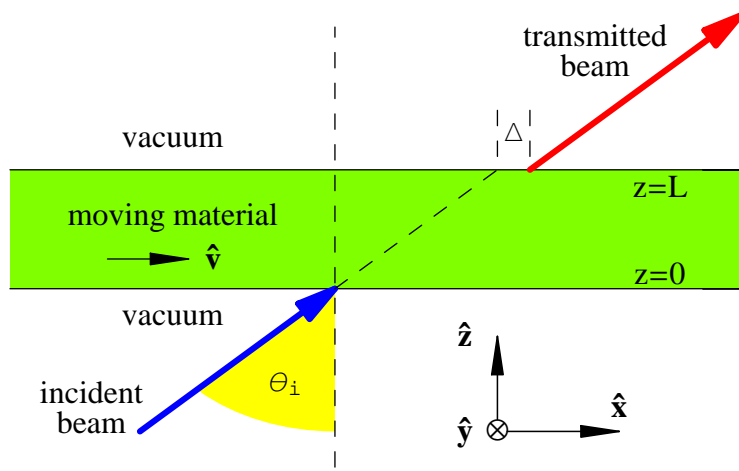


Figure 3: A beam is incident onto a simply moving slab at an angle θ_i with respect to the unit vector \hat{z} normal to the planar interface. The moving material is characterized by relative permittivity $\epsilon_r > 0$ in a comoving frame of reference. As observed in the non-comoving (laboratory) frame of reference wherein the incident plane wave is specified, the transmitted beam is shifted by Δ , parallel to \hat{x} , relative to its position if the slab were absent.

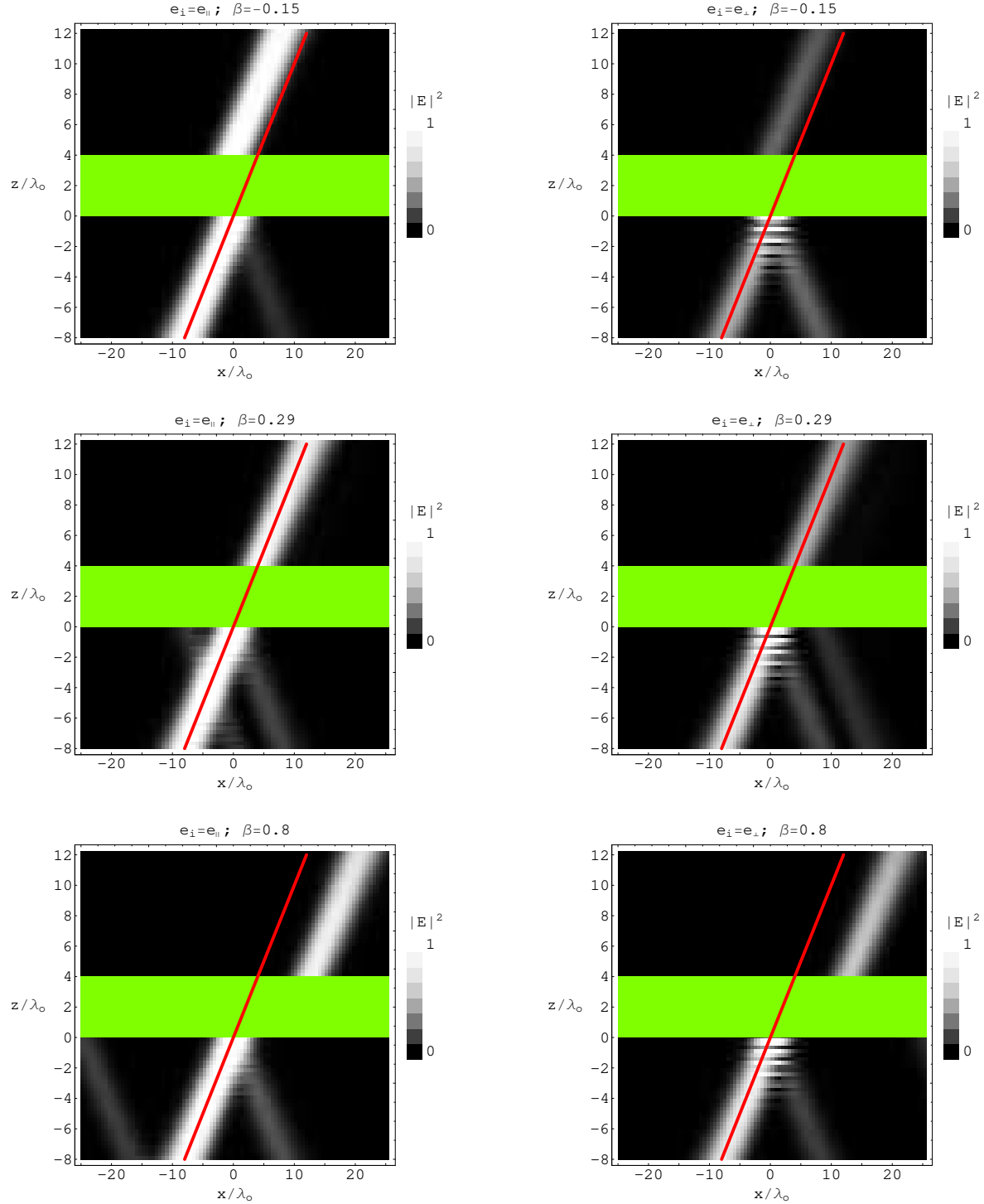


Figure 4: Normalized $|\mathbf{E}|^2$ is mapped in the xz plane for a 2D Gaussian beam incident onto a simply moving slab at an angle $\theta_i = 45^\circ$. The relative speed of the slab is: $\beta = -0.15$ (top); $\beta = 0.29$ (middle); and $\beta = 0.8$ (bottom). The electric field phasor of the incident beam is polarized parallel (left) and perpendicular (right) to the plane of incidence. The red line indicates the mean beam position in the absence of the moving slab.

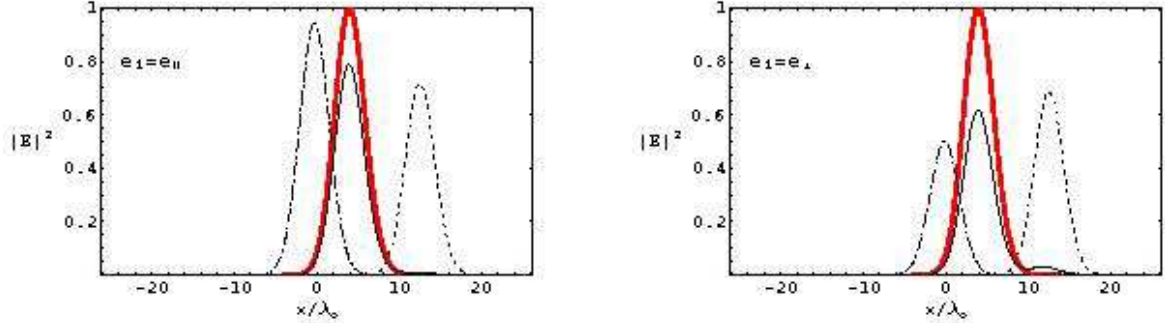


Figure 5: Normalized $|\mathbf{E}|^2$ at $z = 4\lambda_0$ for $\beta = -0.15$ (broken dashed curve); $\beta = 0.29$ (solid dark curve); and $\beta = 0.8$ (dashed curve). The solid red curve represents the normalized $|\mathbf{E}|^2$ in the absence of the moving slab. The electric field phasor of the incident beam is polarized parallel (left) and perpendicular (right) relative to the plane of incidence.

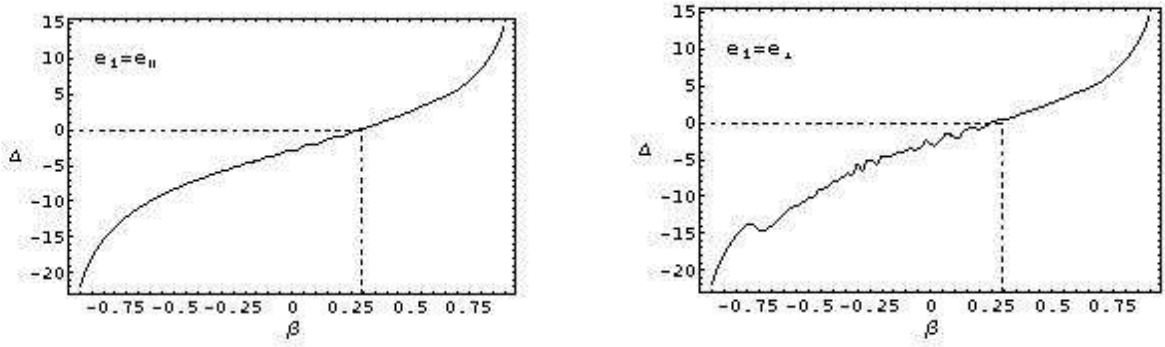


Figure 6: The median beam shift Δ at $z = 4\lambda_0$, plotted against β . The electric field phasor of the incident beam is polarized parallel (left) and perpendicular (right) relative to the plane of incidence. Zero median beam shift at $\beta = 0.29$ is indicated by dashed lines.